REVIEW

Catalytic Reduction of CO$_2$ to CO via Reverse Water Gas Shift Reaction: Recent Advances in the Design of Active and Selective Supported Metal Catalysts

Min Zhu[1,2,3] · Qingfeng Ge[4] · Xinli Zhu[1,2,3]

Abstract

The catalytic conversion of CO$_2$ to CO via a reverse water gas shift (RWGS) reaction followed by well-established synthesis gas conversion technologies may provide a potential approach to convert CO$_2$ to valuable chemicals and fuels. However, this reaction is mildly endothermic and competed by a strongly exothermic CO$_2$ methanation reaction at low temperatures. Therefore, the improvement in the low-temperature activities and selectivity of the RWGS reaction is a key challenge for catalyst designs. We reviewed recent advances in the design strategies of supported metal catalysts for enhancing the activity of CO$_2$ conversion and its selectivity to CO. These strategies include varying support, tuning metal–support interactions, adding reducible transition metal oxide promoters, forming bimetallic alloys, adding alkali metals, and enveloping metal particles. These advances suggest that enhancing CO$_2$ adsorption and facilitating CO desorption are key factors to enhance CO$_2$ conversion and CO selectivity. This short review may provide insights into future RWGS catalyst designs and optimization.

Keywords Carbon dioxide · Reverse water gas shift reaction · Methanation · Supported metal catalyst · Mechanism

Introduction

The concentration of carbon dioxide (CO$_2$) in the atmosphere has increased dramatically, triggering a series of severe environmental problems, such as global warming, glacier melting, and ocean acidification [1–5]. These problems seriously threaten the human living environment. Therefore, CO$_2$ concentration in the atmosphere must be reduced. Many researchers have tried to solve these problems through carbon dioxide capture and storage (CCS) and carbon dioxide capture and utilization (CCU) [6–10]. However, CCS poses a risk of CO$_2$ leakage and causes unknown effects on the environment [11]. Thus, developing the CCU technology appears to be more meaningful than simply storing CO$_2$ [12, 13].

The conversion of CO$_2$ to CO via a reverse water gas shift (RWGS) reaction [Eq. (1)] has been widely explored because the produced CO can be further converted to valuable chemicals and fuels through well-developed synthesis gas (CO and H$_2$) conversion technologies, such as Fischer–Tropsch (FT) synthesis and methanol synthesis. However, the RWGS reaction is competed by Sabatier reaction or CO$_2$ methanation [Eq. (2)] and methanol formation, resulting in a decreased CO yield [11, 14, 15]. Under atmospheric pressure, the yield of methanol is rather low or absent [16] and thus can be ignored. However, the strongly exothermic methanation reaction is thermodynamically more favored over the mildly endothermic RWGS reaction at low reaction temperatures [17–21]; as such, minimizing the methanation during RWGS becomes a great challenge. Therefore, active RWGS catalysts operated at low temperatures with enhanced CO selectivity and minimized CH$_4$ selectivity should be developed. CO may evolve as an intermediate in the hydrogenation of CO$_2$ to CH$_4$, methanol, and other hydrocarbons [11, 16, 17, 22, 23], so understanding the mechanism of CO formation
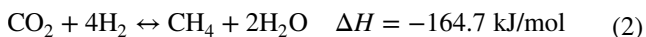
✉ Xinli Zhu
  xinlizhu@tju.edu.cn

1   Key Laboratory for Green Chemical Technology of Ministry of Education, Tianjin University, Tianjin 300350, China

2   Collaborative Innovation Center of Chemical Science and Engineering, Tianjin University, Tianjin 300350, China

3   School of Chemical Engineering and Technology, Tianjin University, Tianjin 300350, China

4   Department of Chemistry and Biochemistry, Southern Illinois University, Carbondale, IL 62901, USA

is also important for the rational design of catalysts for these processes.

$$CO_2 + H_2 \leftrightarrow CO + H_2O \quad \Delta H = 41.3 \text{ kJ/mol} \tag{1}$$

$$CO_2 + 4H_2 \leftrightarrow CH_4 + 2H_2O \quad \Delta H = -164.7 \text{ kJ/mol} \tag{2}$$

Based on reaction kinetics, spectroscopy, and density functional theory (DFT) calculations, two mechanisms of RWGS have been proposed [24–29]. One is redox mechanism: CO_2 is reduced to CO with the catalyst being oxidized directly, and then H_2 reduces the catalyst again to complete the catalytic turnover [24]. This mechanism was originally proposed for Cu-based catalysts, where Cu is oxidized by CO_2 and reduced again by H_2 [24, 25, 30, 31]. This mechanism has also been proposed for catalysts containing reducible oxides, which can be readily reduced and oxidized under reaction conditions [32–36].

Another is association mechanism: CO_2 adsorbs on the surface of catalysts and reacts with dissociated H to form an intermediate species, such as formate (*HCOO), carboxyl (*COOH), carbonate (CO_3^{2-}), and bicarbonate (HCO_3^{-}), which is decomposed to CO and H_2O [27, 37]. This mechanism was originally proposed for metal/reducible support catalysts [27, 38–40], such as Pt/CeO₂. For this mechanism, the key intermediate proposed for the RWGS reaction may vary among different catalysts or the same catalyst operating under different conditions [41–44]. However, redox and association mechanisms have been debated. The mechanism of RWGS reaction is strongly dependent on catalyst types and reaction conditions; as such, no consensus has been reached.

Regardless of the mechanism of the RWGS reaction, an active catalyst requires two functionalities: (a) adsorption of CO_2 and disruption of one C–O bond of CO_2; (b) dissociation of H_2 and hydrogenation of O to form H_2O. A selective RWGS catalyst needs a mild C–O dissociation ability and a weak CO adsorption ability to avoid the dissociation of CO and the further hydrogenation of CO to CH_4 and methanol. Therefore, the balance between C–O dissociation and hydrogenation is a key factor for the development of highly active and selective RWGS catalysts operating under mild conditions. The hydrogenation ability can be provided by a typical transition metal (e.g., Pt and Pd), whereas the C–O breaking ability can be achieved by a mildly oxophilic transition metal (e.g., Ru and Rh) [45–47] and may be further enhanced by a support or a promoter to improve CO_2 adsorption. The balance between hydrogenation and C–O bond dissociation abilities is evidently dependent on the properties and interactions of metals and supports (or promoters).

The development of the RWGS reaction has been briefly reviewed in several reviews focusing on the catalytic conversion of CO_2 to fuels and chemicals [12, 48–50]. For

instance, Porosoff et al. [48] reviewed various catalysts for the conversion of CO_2 to CO, methanol, and hydrocarbon fuels. Kattel et al. [51] reviewed the conversion of CO_2 to C_1 products of CO, methanol, and methane and focused on the role of the interface of metal/oxide catalysts in these reactions. Two reviews on the RWGS reaction have been conducted [12, 37]. Daza and Kuhn [12] analyzed the feasibility of converting CO_2 to liquid fuels through the RWGS reaction. They also explored the supported metal catalysts and oxide catalysts for RWGS, and their reaction mechanisms. Su et al. [37] reviewed the reaction mechanism and more types of catalysts (supported metal catalysts, mixed oxide catalysts, and transition metal carbide catalysts) for the RWGS reaction.

In contrast to previous reviews providing a detailed overview of various types of catalysts for the RWGS reaction, this short review aims to present the recent advances in strategies developed to improve the selectivity and activity of a RWGS reaction. Although other types of catalysts have been widely studied [52–54], our review focuses on supported metal catalysts, which are the most intensively investigated catalyst for the RWGS reaction. In particular, this review considers the role of a support (or a promoter) and its interaction with transition metals in tuning the activity and selectivity of the RWGS reaction.

Strategies to Improve the Activity and Selectivity of the RWGS Reaction

Supported transition metal catalysts have been widely explored for CO_2 reduction. Depending on metal properties, Pd- and Pt-based catalysts are selective for producing CO, whereas catalysts based on oxophilic metals, such as Ni, Rh, and Ru, are more selective for producing CH_4 [55–59]. CH_4 can be a minor or major product under a RWGS reaction condition in the presence of these catalysts [55–59]. Thus, in addition to improving activities, tuning the selectivity of catalysts toward the RWGS reaction is important.

Transition metals, such as Pd and Pt, are highly active for activating H_2. However, they weakly adsorb and activate CO_2. Although DFT work has shown that CO_2 electrochemical reduction by H_2 on Pt (111) is possible [60], Kattel et al. [58] theoretically demonstrated that even a Pt nanoparticle (Pt_{46} cluster) with low coordination surface sites is unable to catalyze the RWGS reaction because of a weak CO_2 adsorption. Kinetic Monte Carlo simulations have revealed that CO production is possible only when the CO_2 adsorption strength is further improved (Fig. 1a), and the weak adsorption of CO facilitates CO desorption while strong adsorption of CO produces more CH_4 (Fig. 1b) [58]. In addition, Kwak et al. [61] experimentally showed that even Pd atomically dispersed on a multiwall carbon nanotube (Pd/MWCNT) is
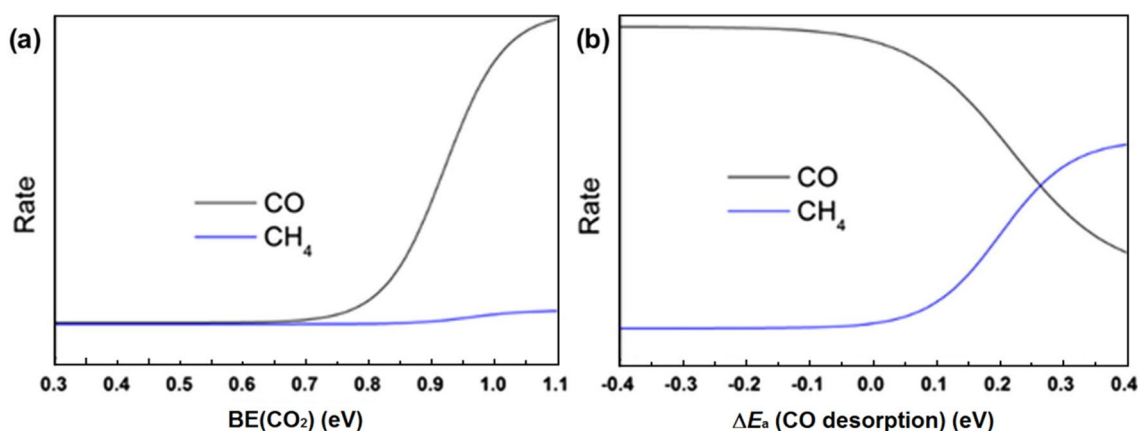
Fig. 1 Sensitivity of CO and CH_4 production rate on the variation in **a** CO_2 binding energy [BE (CO_2)] and **b** CO desorption energy on Pt nanoparticles [58]

inactive (Table 1) for CO_2 reduction under mild conditions (< 500 °C) because neither Pd nor MWCNT can strongly adsorb and activate CO_2 under their reaction conditions. These works have indicated that bare transition metals are inefficient for the RWGS reaction because of their low abilities in CO_2 activation. Therefore, a support or a promoter and its interaction with a transition metal are essential for tuning the activity and selectivity of the RWGS reaction.

Varying Support

The reducibility and acid–base properties of a support can greatly influence reaction intermediates and CO_2 adsorption and activation. Hence, supports play an important role in the activity and selectivity of the RWGS reaction. Choosing an appropriate support is important to tune the activity and selectivity of this reaction.

SiO$_2$ and Al_2O_3 are irreducible supports. Their major role is to disperse the supported species, and they are not expected to directly activate CO_2. Even though SiO_2 is considered an inert support, it can play a role in the RWGS reaction. As shown in Fig. 2a, CO_2 adsorbs at the interface of Pt/ SiO_2; in particular, C adsorbs on Pt, and O bonds with the hydroxyl of SiO_2 via hydrogen bonding [58]. The adsorption strength of CO_2 in the presence of SiO_2 enhances by 0.21 eV compared with that of a bare Pt nanoparticle, thus enabling the RWGS reaction [58]. Al_2O_3 is another widely used irreducible support with weak acidity. In comparison with Pd/MWCNT, which cannot catalyze the RWGS reaction, 0.5% Pd atomically dispersed on Al_2O_3 converts CO_2 to CO and yields CH_4 as a minor product (Table 1) [61]. Using operando diffuse reflectance infrared Fourier transformed spectroscopy (DRIFTS), Bobadilla et al. [62] suggested that CO_2 reacts with the hydroxyl of Al_2O_3 to form bicarbonate species (Fig. 3a), which then reacts with H spilled over from

Au to form formate. Formate eventually decomposes to CO. These studies have indicated that SiO_2 and Al_2O_3 indirectly participate in the RWGS reaction by enhancing CO_2 adsorption. Normally, the activities of SiO_2- and Al_2O_3-supported catalysts in a RWGS reaction are relatively low (Table 1), and they are mainly used to benchmark the activity of supported metals.

In contrast to SiO_2 and Al_2O_3, TiO_2 and CeO_2 are reducible supports, which readily generate oxygen vacancies, particularly in the presence of a metal to activate H_2. An oxygen vacancy participates in a RWGS reaction through the strong adsorption of CO_2 and may directly activate CO_2. Although different reaction pathways are proposed, the oxygen vacancy in proximity to a metal site plays a crucial role in enhancing the activity of the RWGS reaction.

The activity of metal catalysts supported on TiO_2 is normally higher in a RWGS reaction than that on an irreducible support. Kim et al. [32] conducted a kinetic study and proposed that a RWGS reaction follows a redox mechanism on Pt/TiO_2 catalysts. They performed H_2 temperature-programmed reduction and temperature-programmed desorption experiments and suggested that Pt–O_v–Ti^{3+} sites, in addition to Pt and TiO_2 sites, are active sites for a RWGS reaction [32]. The turnover frequency (TOF) of CO_2 conversion on reducible Pt/TiO_2 improves by approximately eight times compared with that on irreducible Pt/Al_2O_3 (Table 1) [32]. Kattel et al. [58] carried out DFT calculation and indicated that CO_2 adsorbs at the interface of Pt/TiO_2 (Fig. 2b); C adsorbs on Pt, and one O adsorbs on an oxygen vacancy (coordinatively unsaturated Ti cation), resulting in an enhanced CO_2 adsorption by 0.11 eV compared with that on Pt/SiO_2. This process facilitates the cleavage of the C–O bond to form the adsorbed CO and fill the oxygen vacancy. Their experimental work has further confirmed that the stronger CO_2 adsorption on Pt/TiO_2 than that on

Table 1 Conditions and catalytic performance of a RWGS reaction on different kinds of catalysts

Catalysts	H_2: CO_2 ratio	Temperature (°C)	Pressure (MPa)	Conversion (%)	Selectivity (%)	Reaction rate [mol/(g_{cat} h)]	TOF (s^{-1})	References
Pt/SiO_2	2:1	300	0.1	3.35	100	—	0.579	[58]
Pt/TiO_2	2:1	300	0.1	4.51	99.08	—	2.760	[58]
1%Pd/MWCNT	3:1	400	—	~ 0	—	~ 0	—	[61]
0.5% Pd/Al_2O_3	3:1	400	—	~ 19	~ 70	~ 0.028	—	[61]
1%Pd-La_2O_3/MWCNT	3:1	400	—	~ 20	~ 100	~ 0.03	—	[61]
Au/Al_2O_3	4:1	400	—	~ 11	—	0.068	—	[62]
Au/TiO_2	4:1	400	—	~ 35	—	0.218	—	[62]
Pt/Al_2O_3	1.4:1	300	0.1	~ 5	—	0.005	~ 0.010	[32]
Pt/TiO_2	1.4:1	300	0.1	~ 10	—	0.010	~ 0.100	[32]
Pt/CeO_2-500	1:1	300	0.1	6.7	—	0.037	0.056	[38]
Cu/SiO_2	3:1	300	0.1	~ 6	98	0.001	0.0006	[63]
Cu/CeO_2	3:1	300	0.1	~ 18	~ 100	0.006	0.0024	[63]
Au/TiO_2	3:1	250	0.8	16.1	93.2	0.009	—	[64]
Au/CeO_2	3:1	250	0.8	3.4	94.8	0.002	—	[64]
Au/ZrO_2	3:1	250	0.8	9.2	96.7	0.005	—	[64]
Pt–Co/TiO_2	2:1	300	—	8.2	98.84	0.041	0.588	[65]
Pt–Co/CeO_2	2:1	300	—	9.1	92.31	0.045	0.335	[65]
Pt–Co/ZrO_2	2:1	300	—	7.8	89.47	0.039	0.267	[65]
5%Ru/Al_2O_3	3:1	350	—	~ 52	~ 98.1	~ 0.078	—	[66]
0.1%Ru/Al_2O_3	3:1	350	—	~ 2	~ 84	~ 0.003	—	[66]
0.7%Ir/CeO_2	4:1	300	1.0	2.9	> 99	0.198	0.020	[67]
5%Ir/CeO_2	4:1	300	1.0	6.8	> 99	0.511	—	[67]
20%Ir/CeO_2	4:1	300	1.0	8.8	12	1.843	—	[67]
Ni/TiO_2	4:1	360	0.1	5.0	100	0.006	—	[57]
Ni/TiO_2-NH_3	4:1	360	0.1	58.2	~ 10	0.072	—	[57]
Ni_3-Fe_3/ZrO_2	2:1	400	0.1	38.8	12.9	0.048	0.613	[68]
Ni_3-Fe_9/ZrO_2	2:1	400	0.1	18.6	95.8	0.023	0.363	[68]
Pd/SiO_2	1:1	600	0.1	29.39	81.6	0.146	—	[59]
Pd-In/SiO_2	1:1	600	0.1	9.57	100	0.048	—	[59]
Cu/SiO_2	1:1	600	0.1	5.3	—	0.329	—	[69]
Cu-1.9%K/SiO_2	1:1	600	0.1	12.8	—	0.796	—	[69]
Pt/mullite	1:1	340	0.1	~ 2.4	~ 96	0.013	0.080	[70]
Pt-K/mullite	1:1	340	0.1	~ 8	~ 100	0.045	0.560	[70]
Rh-Y	3:1	250	3	24.1	0.3	0.015	0.016	[71]
Rh-10Li/Y	3:1	250	3	13.1	86.6	0.008	0.017	[71]
Rh/S-1	3:1	300	1	6.6	85.7	0.00002	—	[72]
Rh@HZSM-5	3:1	300	1	18.1	~ 0	0.00016	—	[72]
Rh@S-1	3:1	300	1	4.9	92.6	0.00001	—	[72]

Pt/SiO_2 improves the TOF of CO_2 conversion in the RWGS reaction by 4–5 times (Table 1) [58]. Bobadilla et al. [62] reported that the activation energy of a RWGS reaction on Au/TiO_2 is 30 kJ/mol, which is much lower than that of 79 kJ/mol on Au/Al_2O_3; as a result, the RWGS activity on Au/TiO_2 is higher than that on Au/Al_2O_3. As shown in Fig. 4, under identical reaction conditions (0.2 g of catalyst, H_2/CO_2 = 4/1, gas hourly space velocity [GHSV] is 12,000 h^{-1}), the conversion of CO_2 for Au/TiO_2 approaches the thermodynamic equilibrium of CO_2 conversion, while it is much lower on Au/Al_2O_3 (Table 1) [62]. Bobadilla et al. [62] further performed DRIFTS and UV–vis spectroscopy studies and proposed that the presence of oxygen vacancies (or Ti^{3+} cations) during the reaction facilitates the formation of a surface hydroxycarbonyl (OCOH) intermediate, which decomposes to form CO and H_2O (Fig. 3b).
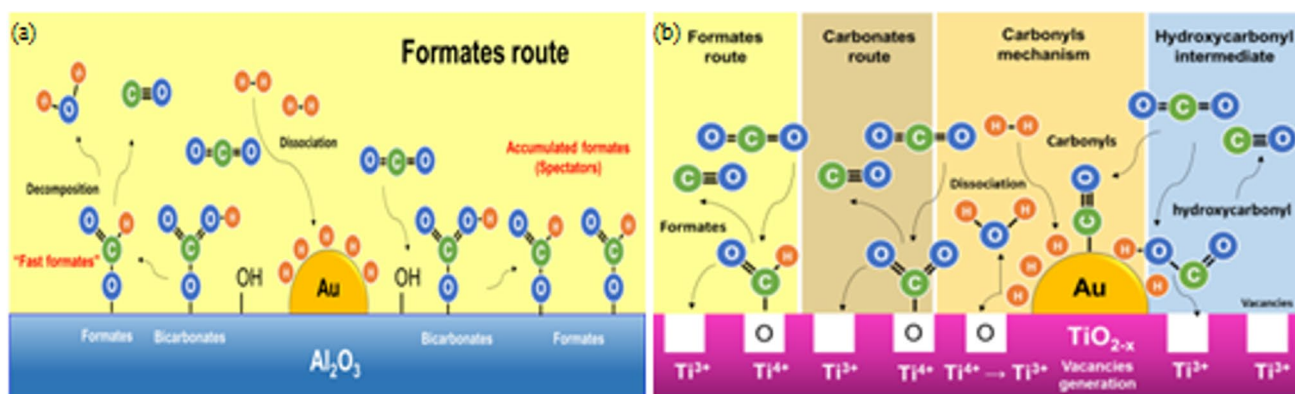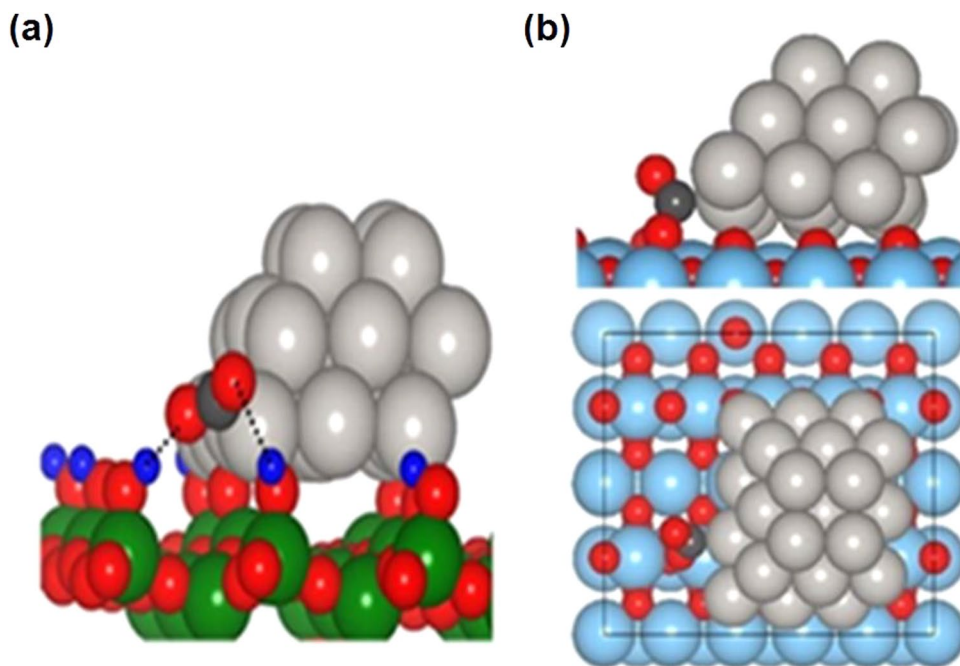
Fig. 3 Proposed mechanism of the RWGS reaction on **a** Au/Al$_2$O$_3$ and **b** Au/TiO$_2$ catalysts based on the results of DRIFTS and UV–Vis. Reaction conditions: H_2/CO_2 = 4/1, 150–450 °C, feed flow rate 10–50 mL/min [62]

CeO_2 is also a reducible support whose oxygen storage capacity (OSC) is higher than that of TiO_2. CeO_2-supported transition metal catalysts have been widely investigated for the mechanism of a RWGS reaction under various conditions [27, 73, 74]. An early work showed that CO_2 adsorption on Pt/CeO_2 at room temperature produces CO adsorbed on Pt and suggested that an oxygen vacancy in the vicinity of a Pt particle is responsible for CO_2 reduction to CO [75]. Performing DRIFT and mass spectroscopy (MS) during steady-state isotopic transient kinetic analysis, Goguet et al. [27] suggested that surface carbonate is an active intermediate, and formate is a spectator during the RWGS reaction on Pt/CeO_2 under their reaction condition. Wang et al. [74] conducted a quantitative transient analysis of products and

showed that the surface oxygen vacancy in the vicinity of a Au particle in Au/CeO_2 can be replenished by an interaction with CO_2 and proposed that the RWGS reaction may follow a redox mechanism via the Au-assisted deposition and removal of active surface O. They also compared the OSC properties of Au/CeO_2 and Au/TiO_2 and suggested that oxygen vacancies away from an Au particle may be involved in the RWGS reaction on Au/CeO_2, because of the higher oxygen mobility in CeO_2 than in TiO_2. However, Chen et al. [38] combined Fourier transform infrared (FTIR) experiments and a temperature-programmed surface reaction and proposed that redox and associate mechanisms exist on a Pt/ CeO_2 catalyst via a related mechanism that involves a surface formate species as the major path under their reaction
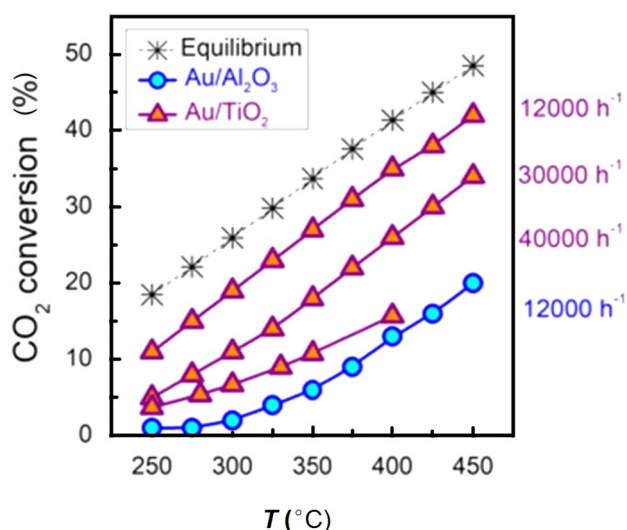
Fig. 4 The catalytic performance of Au/TiO$_2$ and Au/Al$_2$O$_3$ catalysts in the RWGS reaction. Reaction conditions: 0.2 g catalyst, H$_2$/CO$_2$=4/1, feed flow rate 50 mL/min, and gas hourly space velocity (GHSV) from 12,000 to 40,000 h^{-1} [62]

condition. These works have indicated that oxygen vacancies play an important role in the RWGS reaction, even though its reaction mechanism may vary depending on reaction conditions.

The RWGS activity of transition metals on CeO$_2$ is higher than that of metals supported on irreducible supports. Porosoff and Chen [76] compared the RWGS reaction on 1.7% Pt supported on reducible CeO$_2$ and irreducible Al$_2$O$_3$ at 573 K (H$_2$/CO$_2$ = 3/1, total pressure 30.0 Torr) and found that the forward reaction rate constant based on the mass of a catalyst and the amount of CO uptake (a measure of Pt metal dispersion) on Pt/CeO$_2$ are ~ 1.7 and ~ 5.7 times higher than those on Pt/Al$_2$O$_3$ [76]. Yang et al. [63] prepared ~ 2 nm Cu supported on CeO$_2$ and mesoporous SiO$_2$ to exclude the effect of the particle size of Cu. They observed that Cu/CeO$_x$ is about four times more active than Cu/SiO$_2$ at 573 K (Table 1; 0.2 g of catalyst, H$_2$/CO$_2$ = 3/1, 1 bar, weight hourly space velocity of 1.08 h^{-1}) and assigned this improvement to the formation of oxygen vacancies on the Cu/CeO$_x$ catalyst.

In summary, the activity of metal catalysts on reducible supports (CeO$_2$ and TiO$_2$) in a RWGS reaction is higher than that on irreducible supports (SiO$_2$ and Al$_2$O$_3$; Table 1), but they may form more CH$_4$. No CH$_4$ forms on Au- and Cu-based catalysts, whereas CH$_4$ may form on Pt and Pd catalysts [62, 63]. For Pt catalysts, CH$_4$ selectivity is higher on reducible supports (TiO$_2$ and CeO$_2$) than on irreducible supports (SiO$_2$ and Al$_2$O$_3$) possibly because of the removal of both O atoms from CO$_2$ by oxygen vacancies and the hydrogenation of the formed C species to CH$_4$ [76]. The deposited carbon species on a support may lead

to catalyst deactivation. Indeed, Goguet et al. [73] reported the deactivation of a 2% Pt/CeO$_2$ catalyst during a RWGS reaction. They subjected the used catalysts to temperature-programmed oxidation and found that deactivation is closely related to the amount of deposited carbon. Thus, carbon species deposited on partially reduced CeO$_2$ around a Pt particle is the major reason for this deactivation.

Although metal/reducible support catalysts show higher activity in RWGS, the work of direct comparison between different reducible supports and their consequences on the varied activity and selectivity for RWGS reaction is rare. Sakurai et al. [64] studied CO$_2$ hydrogenation on Au/CeO$_2$, Au/ZrO$_2$, and Au/TiO$_2$ catalysts. Under identical reaction conditions [250 °C, H$_2$/CO$_2$ = 3, 8 atom pressure, 3000 mL/(g$_{cat}$ h)], these catalysts show similar CO selectivity (> 90%), whereas conversion is quite different: 3.4%, 9.2%, and 16.1% for Au/CeO$_2$, Au/ZrO$_2$, and Au/TiO$_2$, respectively (Table 1). This high activity on Au/TiO$_2$ is attributed to the higher acidity of TiO$_2$ than those of ZrO$_2$ and CeO$_2$. Kattel et al. [65] compared CO$_2$ hydrogenation on bimetallic PtCo supported on CeO$_2$, ZrO$_2$, and TiO$_2$. Similar CO$_2$ conversion (7.8%–9.1%) is observed on these catalysts under identical condition (0.1 g of catalyst, 300 °C, H$_2$/CO$_2$ = 2/1, feed flow rate of 60 mL/min), whereas the highest TOF and the highest CO selectivity are found on a PtCo/TiO$_2$ catalyst (Table 1). These ascribed this change to the strength of C, O-bound, and O-bound species are enhanced on PtCo/CeO$_2$ and PtCo/ZrO$_2$ interfaces with respect to that of PtCo/TiO$_2$. As a result, different reaction intermediates form, and CH$_4$ selectivity increases. We note that the surface area of these reducible supports are different, perhaps resulting in a comparison with different bases. Therefore, how the redox and acid–base properties of different supports influence the activity and selectivity of RWGS reaction should be further studied.

Tuning Metal–Support Interactions

A RWGS reaction occurs at the interface of a metal and a support, so finely tuning metal–support interactions and maximizing metal–support interfacial sites can greatly improve activity and enhance selectivity toward CO. Maximizing metal–support interfacial sites can be achieved by reducing the particle size of metals, adjusting pretreatment procedures, and tuning the property of supports. Tuning metal–support interactions is particularly important for Ni-, Rh-, and Ru-based catalysts, which are more selective to the production of CH$_4$ rather than CO.

Reducing the particle size of transition metals not only provides more surface sites for a reaction but also increases the number of metal–support interfacial sites and has been investigated by several groups. Kwak et al. [66] tested CO$_2$ hydrogenation on 0.1%–5% Ru/Al$_2$O$_3$ catalysts. CH$_4$ is the

major product on a 5% Ru sample (mainly Ru particles), while CO is the major product on a 0.1% Ru sample (mainly atomically dispersed Ru; Table 1). On the 0.1% Ru/Al$_2$O$_3$ catalyst at 350 °C (Fig. 5), CO is the only product at the beginning of a reaction, whereas CH$_4$ becomes the major product with time on stream. This is because the sintering of atomically dispersed Ru on particles occurs with time on stream possibly due to a weak Ru–Al$_2$O$_3$ interaction. Matsubu et al. [56] prepared 2% Rh/TiO$_2$ catalyst with both Rh particles and isolated Rh sites. They removed the Rh particles without removing isolated Rh species that strongly interacts with TiO$_2$ by leaching with HCl/H$_2$O$_2$ (Fig. 6a). In comparison with a fresh Rh/TiO$_2$ catalyst with Rh particles exhibiting the major product of CH$_4$, the leached Rh/

TiO$_2$ catalyst with only the isolated Rh sites produces CO at 200 °C and CO$_2$/H$_2$ of 3 (15–30 mg of catalyst, 0.1 MPa, CO$_2$/H$_2$/N$_2$ = 3/1/96, feed flow rate of 100 mL/min; Fig. 6). Therefore, they concluded that an isolated Rh site is the active site for a RWGS reaction, while Rh particle is the active site for CH$_4$ formation. Combining DFT and experiments, Chen et al. [77] also demonstrated that a single Ir atom interacting with TiO$_2$ is selective for CO formation, whereas Ir particle is active for CH$_4$ formation. These works have mainly focused on the particle size of metals but have rarely explored the role of metal–support interactions.

However, one may expect that metal–support interactions can be enhanced by decreasing the particle size of metals because of an increased metal–support interface. Recently,
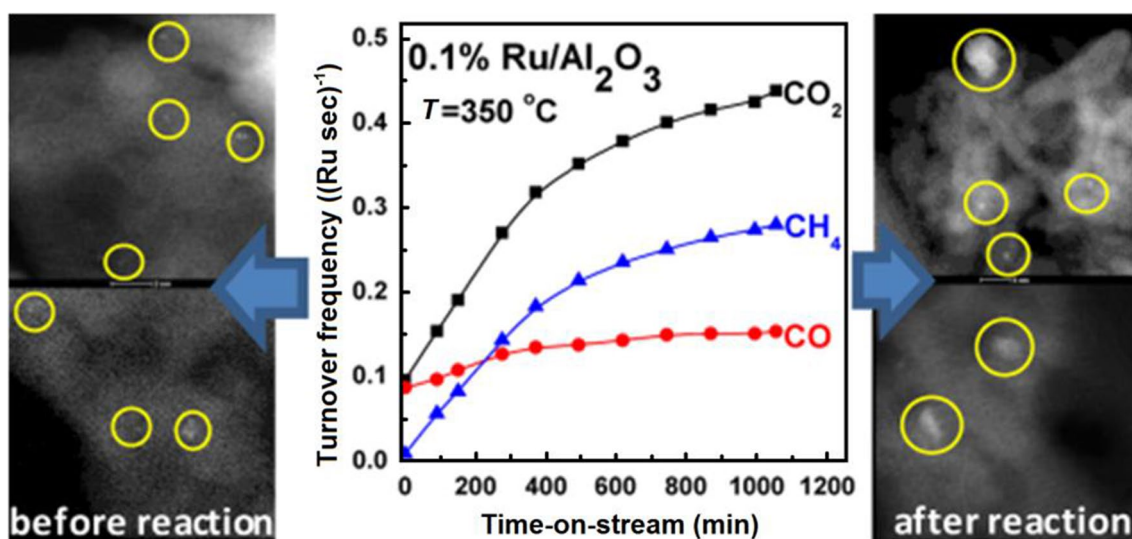

Fig. 5 Effect of time on stream on the turnover frequency (TOF) of CO$_2$ conversion, CH$_4$ and CO formation on 0.1% Ru/Al$_2$O$_3$ during CO$_2$ reduction, and the STEM images of the catalyst before and after reaction. Reaction conditions: 350 °C, 0.05 g of catalyst, H$_2$/CO$_2$/He = 3/1/16, feed flow rate of 60 mL/min [66]
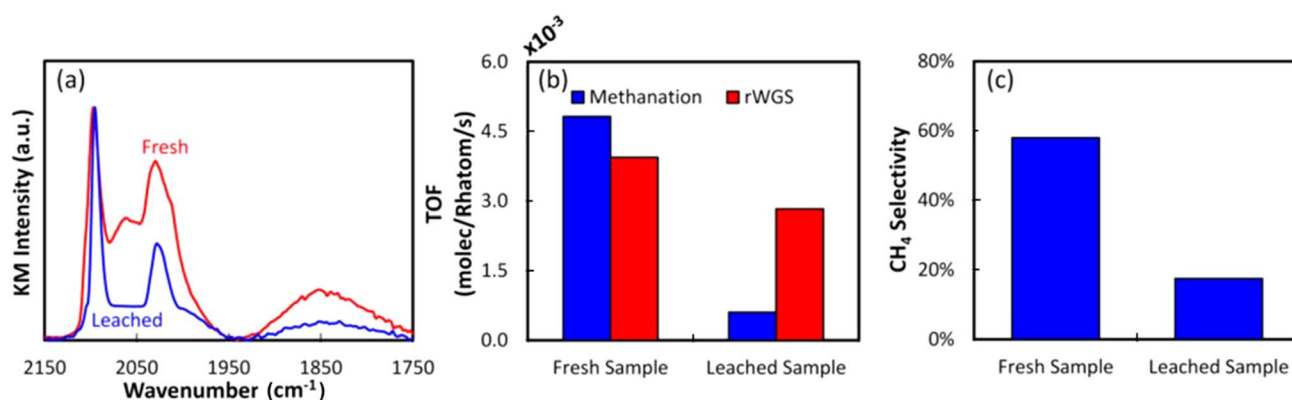

Fig. 6 **a** DRIFTS spectra of CO adsorption on fresh 2% Rh/TiO$_2$ and HCl/H$_2$O$_2$-leached Rh/TiO$_2$ samples, showing Rh particles were leached; **b** TOF of methanation and RWGS reactions, and **c** CH$_4$ selectivity on the fresh 2% Rh/TiO$_2$ and leached samples. Reaction conditions: 200 °C, 0.1 MPa, CO$_2$/H$_2$/N$_2$ = 3/1/96, feed flow rate of 100 mL/min [56]

Li et al. [67] prepared 5% Ir/CeO_2 catalyst with an Ir particle size of approximately 1 nm and 0.7% Ir/CeO_2 with atomically dispersed Ir. Although an Ir/CeO_2 catalyst with large Ir particles (> 2.5 nm) shows the dominant product of CH_4, the 5% and 0.7% Ir/CeO_2 catalysts have the dominant product of CO. The activity based on the mole of Ir improves when the size of an Ir particle is smaller than 1 nm (Table 1; 300 °C, 1 MPa, $H_2/CO_2/Ar = 76/19/5$). Li et al. [67] also conducted X-ray adsorption spectroscopy (XAS) and found that 1 nm Ir particle and atomically dispersed Ir become partially oxidized because of the strong interaction with CeO_2, whereas a large Ir particle (> 2.5 nm) is mainly reduced. Thus, they argued that the main active site for a RWGS reaction is the partially oxidized Ir that strongly interacts with CeO_2 support irrespective of Ir particles or atomically dispersed Ir species.

Varying treatment conditions can tune the metal–support interactions of metal/reducible support catalysts. Aitbekova et al. [55] prepared ~ 2.6 nm Ru uniformly dispersed on Al_2O_3, TiO_2, and CeO_2 supports and tested in a CO_2 reduction reaction. They found that TiO_2- and CeO_2-supported Ru are more active than Al_2O_3-supported Ru catalyst and that CH_4 is the major product in all catalysts. However, the mild oxidation of catalysts at 230 °C and followed by low-temperature (230 °C) reduction results in the redispersion of Ru particles to form a single RuO_x site on CeO_2, which causes an almost complete shift of the product selectivity from CH_4 to CO (Fig. 7). This enhanced selectivity is attributed to the weakened adsorption of CO on the single RuO_x site. However, this redispersion partially occurs in Al_2O_3- and TiO_2-supported Ru possibly because of the weaker interaction of Al_2O_3 and TiO_2 than that of CeO_2 with RuO_x to disperse the single RuO_x site. The mild oxidation at 230 °C and followed by the high-temperature (500 °C) reduction of Ru/TiO_2 favor the formation of a strong metal–support interaction (SMSI). That is, the partially reduced TiO_x covers Ru particles, resulting in a decreased CO_2 conversion
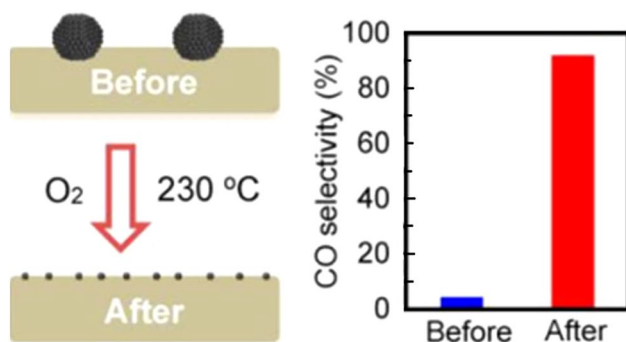
and an enhanced CO selectivity due to the loss of a surface Ru site by covering. Interestingly, the redispersed Ru/CeO_2 catalyst via a mild oxidizing treatment is stable in a RWGS reaction for 12–14 h, and CO selectivity increases further from 90% to 99%. Similarly, the high-temperature (500 °C) reduction of a Ni/TiO_2 catalyst results in a SMSI effect with a decreased activity, but this reaction shifts the selectivity from CH_4 to CO (Table 1) because Ni is covered, and more $Ni–TiO_2$ interface sites are produced [57]. However, for the supported Ni catalysts prepared from NH_3 or H_2-pretreated TiO_2 support, reduction at 500 °C only induces a SMSI effect to a limited extent; thus, CH_4 is the dominant product on these catalysts (Table 1).

In addition to changing metal particle sizes or pretreatment conditions, varying the property of a support can also be used to tune metal–support interactions. Kim et al. [78] prepared a series of Pt/TiO_2 catalysts with a varying crystallite size of TiO_2. They found that decreasing the crystallite size of TiO_2 significantly improves the reducibility of Pt/TiO_2, produces more $Pt–Ov–Ti^{3+}$ interfacial sites, and eventually improves the activity in a RWGS reaction (Fig. 8).

Addition of Reducible Transition Metal Oxide Promoters

The addition of a promoter can also change the adsorption and activation of CO_2 and may further change the activity and selectivity for a RWGS reaction. One type of a promoter is reducible transition metal oxide, which can also form oxygen vacancies upon reduction. Similar to oxygen vacancies on reducible TiO_2 and CeO_2, oxygen vacancies at the interface of a metal-reducible metal oxide promoter may play an important role in CO_2 activation. Adjusting the interaction
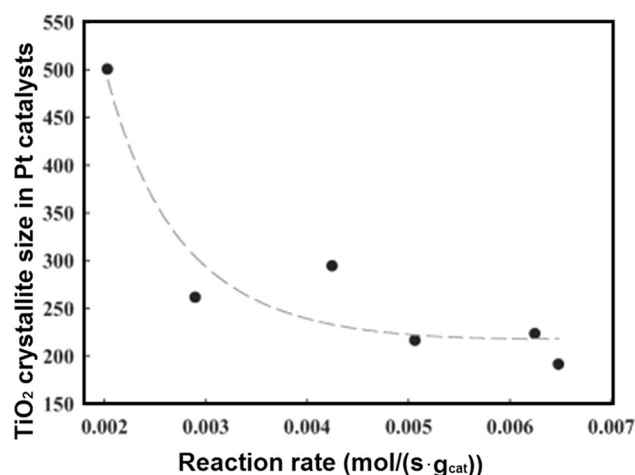

Fig. 7 Schematic of oxygen treatment at 230 °C on the structure of Ru/CeO_2 catalyst and its effect on CO selectivity during CO_2 reduction reaction. Reaction conditions: 0.02 g of catalyst, 240 °C, 0.1 MPa, $H_2/CO_2 = 4/1$ [55]

Fig. 8 Effect of the primary crystallite size of TiO_2 support on the rate of the RWGS reaction on Pt/TiO_2 catalysts. Reaction conditions: 0.5 g of catalyst, 300 °C, feed gas flow rate of 100 mL/min [78]

between a metal and a promoter may significantly improve the activity and tune selectivity in a RWGS reaction.

Kwak et al. [61] compared the CO_2 reduction on 1% Pd/ MWCNT and 1% Pd-2.3% La_2O_3/MWCNT catalysts (0.05 g of catalyst, $H_2/CO_2/He = 3/1/16$, feed flow rate of 60 mL/ min). In contrast to the inactivity of 1% Pd/MWCNT for CO_2 reduction, addition of La_2O_3 to the catalyst improves the activity, and CO is observed as the only product (< 500 °C; Table 1). This observation highlights the role of La_2O_3 in CO_2 activation. Ro et al. [79] prepared a MoO_x-modified Pt/SiO_2 catalyst via a controlled surface reaction. MoO_x is selectively deposited on surface Pt at a Mo/Pt ratio of < 0.3, thereby creating Pt–MoO_x interfacial sites. The intrinsic reaction rate and TOF of the optimized PtMo/SiO_2 (Mo/ Pt = 0.3) for the RWGS reaction at 473 K improve by ~ 11 and ~ 39 times compared with those of Pt/SiO_2 (Fig. 9), respectively ($H_2/CO_2 = 2$, 7.1 bar). The activation energy decreases from 67.9 kJ/mol for Pt/SiO_2 to 60.0 kJ/mol for PtMo/SiO_2. The reaction orders are altered upon MoO_x loading. Interestingly, the activity of the RWGS reaction can be further improved when Pt-MoO_x is exposed to light irradiation. Yan et al. [68] investigated CO_2 reduction on NiFe/ ZrO_2 catalysts with varying amounts of Fe loadings. As shown in Fig. 10, at low Fe loadings (Ni/Fe > 1), the major active site is the Ni–ZrO_2 interface, which selectively produces CH_4 (selectivity > 88%) through methanation (673 K, $H_2/CO_2/Ar = 2/1/5$). At high Fe loadings (Ni/Fe = 1/3), the major active site is a Ni–FeO_x interfacial site, producing CO with selectivity higher than 95% (Table 1). DFT calculations have indicated that the CO adsorption energies at Ni–ZrO_2
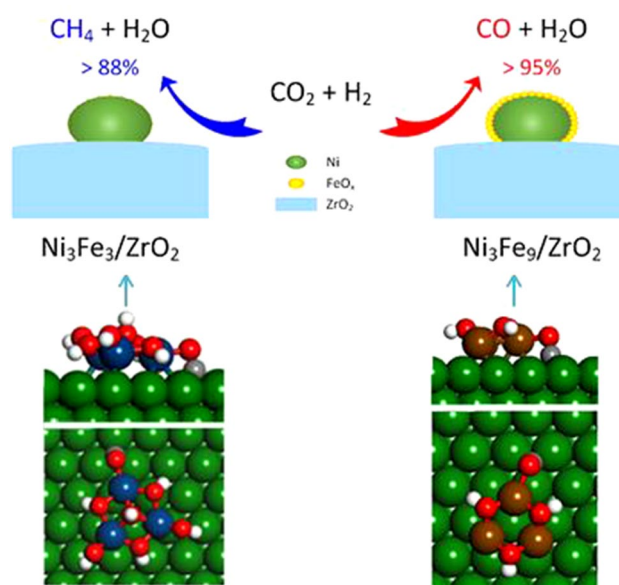

Fig. 10 Structural diagrams and DFT-optimized CO adsorption geometries at the interface sites of Ni_3Fe_3/ZrO_2 and Ni_3Fe_9/ZrO_2 catalysts and their selectivity to CH_4 and CO during CO_2 reduction reaction. Reaction conditions: 0.1 g of catalyst, 400 °C, 0.1 MPa, $H_2/CO_2/$ Ar = 2/1/5, feed flow rate of 40 mL/min [68]

and Ni–FeO_x interfaces are −2.92 and −1.93 eV, respectively. Therefore, CO adsorbed at the Ni–ZrO_2 interface is too strong, so it favors CH_4 formation. Conversely, CO adsorbed at the Ni–FeO_x interface is weaker, so it promotes CO desorption.

Bimetallic Alloy Formation

Another type of promoter can be completely reduced to form a bimetallic alloy with a major metal [80–82]. Depending on the property of promoters, bimetallic alloy properties, such as H_2 dissociation, CO_2 adsorption, and C–O cleavage, may be changed. For example, Yuan et al. [81] performed a DFT study on CO_2 hydrogenation on Ni (111) and Re-doped Ni (111) surfaces. The adsorption energies of CO_2 on Ni (111) and Re@Ni (111) surfaces are 0.20 and −0.28 eV, respectively. This result indicates the stronger adsorption of CO_2 on the latter surface. Furthermore, the activation energy of CO_2 dissociation to CO* and O* decreases from 0.41 eV on Ni (111) to 0.18 eV on Re@Ni (111). These results suggest that the presence of oxophilic Re on Ni (111) favors one O atom of CO_2 adsorption on Re and promotes the C–O bond dissociation. Thus, a bimetallic alloy may also change the activity and selectivity of a RWGS reaction.

Alayoglu et al. [80] showed that Pt is segregated on the surface of a PtCo alloy, and the selectivity of CO increases from ~ 82% on Co/MCF-17 to ~ 100% on PtCo/MCF-17 at a CO_2 conversion of ~ 5% (reaction conditions: 0.05 g of
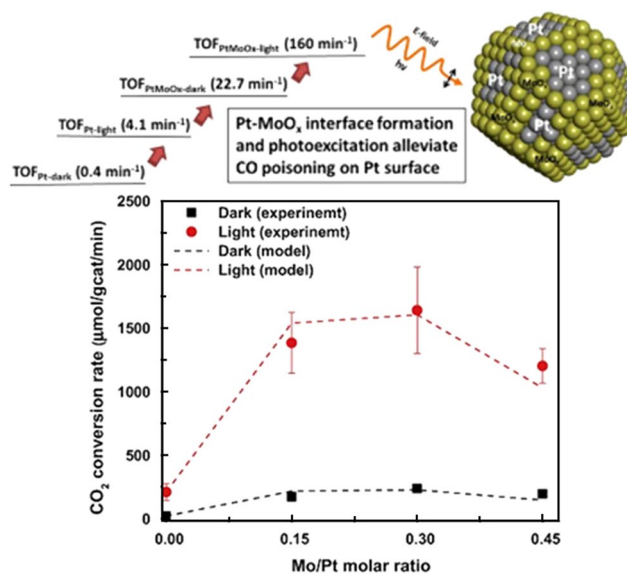

Fig. 9 Turnover frequency (TOF) and reaction rate of RWGS reaction on Pt/SiO_2 and PtMo/SiO_2 catalysts in dark and light conditions at 473 K. Reaction conditions: 200 °C, 0.71 MPa, $H_2/CO_2 = 2/1$, feed flow rate of 15 mL/min. [79]

catalyst, 300 °C, 5.5 bar, $H_2/CO_2/He = 33.3/11.1/5.6$, feed flow rate of 50 mL/min). Porosoff and Chen [76] compared CO_2 reduction on bimetallic PtCo, PtNi, and PdNi supported on Al_2O_3 or CeO_2 catalysts. $PdNi/CeO_2$ is the most active catalyst, but it forms the highest amount of CH_4. By comparison, $PtCo/Al_2O_3$ shows the highest selectivity toward CO. They suggested that selectivity can be correlated with the electronic properties of catalysts by using values of the d-band center. As shown in Fig. 11, the Pt–Co bimetallic catalyst with a d-band center value away from the Fermi level and toward the more negative direction yields the highest CO:CH_4 ratio. The advantage of establishing this trend is that it can provide a direction for the future selection of single-metal or bimetallic catalysts that efficiently activate CO_2. Further studies have indicated that $PtCo/TiO_2$ is more selective than $PtCo/CeO_2$ and $PtCo/ZrO_2$ catalysts for CO because of the weak bonding strength of CO at the Pt–Co/ TiO_2 catalyst interface site [65]. Ye et al. [59] compared CO_2 reduction on Pd/SiO_2 and $PdIn/SiO_2$ catalysts. A Pd/ SiO_2 catalyst is much more active than other catalysts, but it produces CH_4 as a minor product. By comparison, PdIn/ SiO_2 is much less active than other catalysts, but it only produces CO (Table 1). Characterizations have shown the formation of a PdIn bimetallic alloy (Fig. 12). A DFT study has revealed that a PdIn alloy is less active than Pd for H_2 dissociation, CO adsorption on the PdIn alloy is weaker than that on Pd, and PdIn is energetically less favorable to the hydrogenation of CO to CH_4 than Pd. Specifically, the H_2 dissociation energy on a PdIn alloy increases by 1.56 eV, whereas the linear CO adsorption energy on a PdIn alloy decreases by 0.77 eV. These changes shift the formation of CH_4 on Pd/SiO_2 to the formation of CO on bimetallic PdIn/ SiO_2.
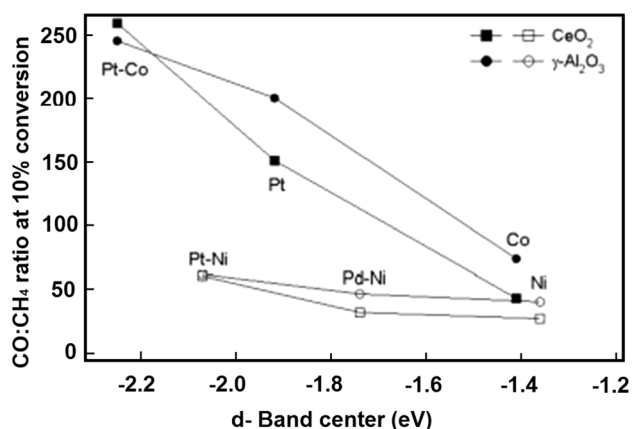

Fig. 11 Effect of the d-band center on the ratio of CO to CH_4 production at 10% conversion of the RWGS reaction. Open and solid symbols represent catalysts with and without Ni, respectively. Reaction conditions: 573 K, 0.004 MPa, $H_2/CO_2 = 3/1$ [76]

Addition of Alkali Metals

The addition of alkali metals to Pt- and Au-based catalysts can greatly improve the activity of a water gas shift (WGS) reaction [83–85]. The addition of an appropriate amount of Na to Pt/TiO_2 can improve reducibility and surface basicity and form strong Pt-O-Na interactions by donating electrons from Pt to NaO_x, which creates an active site at the interface of Pt–NaO_x for the WGS reaction [83]. The increased basicity may improve the adsorption of acidic CO_2. Furthermore, electronically modified Pt may alter interactions with CO, enhance activity, and tune the selectivity for the RWGS reaction.

Chen et al. [69] showed that the addition of a small amount of K_2O to a Cu/SiO_2 catalyst improves its activity for a RWGS reaction by more than 2.4 times (Table 1). Specifically, the CO_2 conversion is 12.8% on a $Cu/K_2O/ SiO_2$ catalyst, while it is only 5.3% on Cu/SiO_2 catalyst at 600 °C (0.02 g of catalyst, 0.1 MPa, $H_2/CO_2 = 1/1$, feed flow rate of 100 mL/min). K likely enhances CO_2 adsorption and facilitates the decomposition of the formate species to CO. Liang et al. [70] studied the effect of the addition of 2% K to 2% Pt/mullite on the RWGS reaction. The TOF of RWGS at 340 °C improves by seven times with the addition of K (Table 1; $H_2/CO_2/N_2 = 4.5/4.5/1$, feed flow rate of 50 mL/ min) with a reduced selectivity to CH_4 (Fig. 13). The activation energy of CO_2 conversion decreases from 62 ± 2.3 kJ/ mol to 34 ± 1.3 kJ/mol upon K addition. This result suggests that the interface between KO_x and Pt serves as an active site for the decomposition of formate to CO, and the presence of KO_x weakens CO adsorption on Pt and thus hinders CH_4 formation. Yang et al. [86] investigated the role of K addition in the activity and selectivity of Pt on zeolite L (Pt/L) for a RGWS reaction. K addition (K/Pt = 80) improves the reaction rate from 0.021 mol/(g_{cat} h) to 0.080 mol/(g_{cat} h) at 500 °C compared with that of Pt/L (0.1 g of catalyst, $H_2/ CO_2/N_2 = 4.5/4.5/1$, feed flow rate of 50 mL/min), while CH_4 formation decreases. On the basis of XAS and X-ray photoelectron spectra (XPS) results, Yang et al. [86] proposed the formation of a Pt–O(OH)–Pt interface, which serves as an active site to adsorb CO_2 and form an active intermediate of bridge-bonded formate. Similarly, Santos et al. [84] reported that the addition of Na to Pt/C can improve the RWGS reaction with a reduced activation energy. They suggested that the addition of Na modifies the electronic structure of Pt and favors CO_2 dissociation.

In addition to improving the activity of the RWGS reaction, changing product selectivity can be achieved by adding alkali metals. Bando et al. [71] investigated the effect of Li modification on Rh-exchanged Y zeolite for CO_2 hydrogenation (1 g of catalyst, 250 °C, 3 MPa, $H_2/CO_2 = 3/1$, feed flow rate of 100 mL/min). They found that CH_4 is the major product of Rh-Y, whereas adding Li to Rh-Y mainly
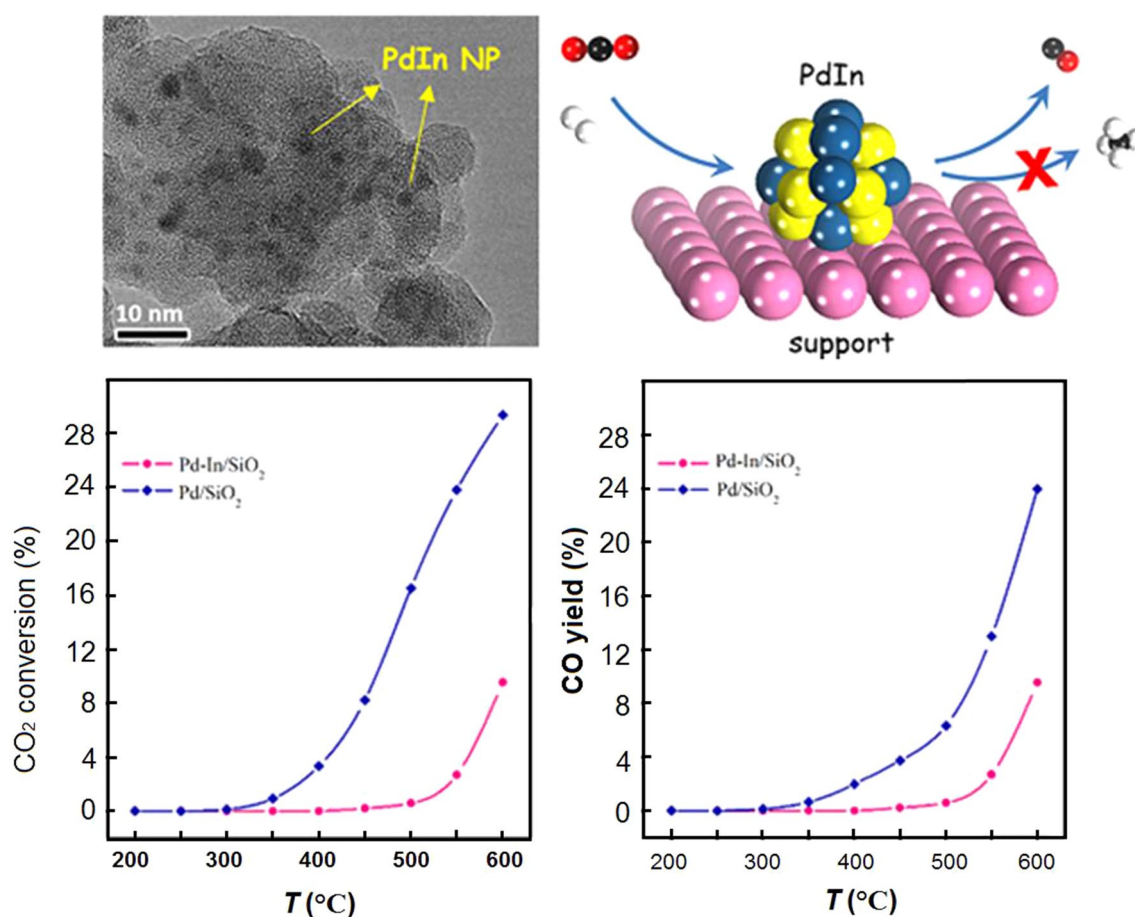
Fig. 12 TEM image of PdIn bimetallic nanoparticles, DFT modeling of PdIn alloy and the catalytic performance of Pd-In/SiO$_2$ and Pd/SiO$_2$ catalysts. Reaction conditions: 0.05 g of catalyst, 600 °C, 0.1 MPa, H$_2$/CO$_2$/Ar = 1/1/3, feed flow rate of 50 mL/min [59]

produces CO (Table 1). This change is attributed to Li that provides new active sites for CO$_2$ adsorption and stabilizes the adsorbed CO.

Enveloping Metal Particles

These above strategies are based on tuning metal–support (promoter) interactions. The local environment of metal particles is also important for various reactions and may be finely tuned by enveloping with nanoporous materials. Wang et al. [72] reported a new strategy to tune the local environment of metals by enveloping a metal particle with different zeolites for CO$_2$ reduction reaction. The Rh particles of 4.2–5.0 nm are either supported on zeolite (Rh/HZSM-5, Rh/S-1) or enveloped in HZSM-5, KZSM-5, and pure silica zeolite of S-1 (Rh@HZSM-5, Rh@KZSM-5, and Rh@S-1). CO$_2$ reduction reaction tests (0.5 g of catalyst, 1 MPa, H$_2$/CO$_2$/Ar = 3/1/1, feed flow rate of 30 mL/min, 250–500 °C) showed that Rh/HZSM-5, Rh/S-1, and Rh@HZSM-5 favor CH$_4$ formation, whereas Rh@S-1 produces CO as a major product (Table 1) and CH$_4$ as a minor product

(Fig. 14). The selectivity behavior of Rh particles enveloped in S-1 is similar to that of the single Rh site on TiO$_2$ [56]. FTIR and H$_2$ spillover experiments showed that proton form HZSM-5 favors stronger CO adsorption on Ru and facilitates hydrogen spillover, while pure silica zeolite favors weaker CO adsorption and limited hydrogen spillover. The weak CO adsorption favors desorption, and the limited hydrogen spillover decreases the Rh hydrogenation ability toward the CH$_4$ formation. A stability test at 400 °C has demonstrated that Rh/S-1 is stable for 150 h with a CO selectivity of 96%.

Conclusions and Outlooks

The catalytic conversion of CO$_2$ to CO via the RWGS reaction followed by well-established synthesis gas conversion technologies may provide a potential approach to convert CO$_2$ to valuable chemicals and fuels. The improvement in the low-temperature activity and selectivity of the RWGS reaction is a key challenge for this reaction. We reviewed recent advances in the strategies of catalyst designs that can
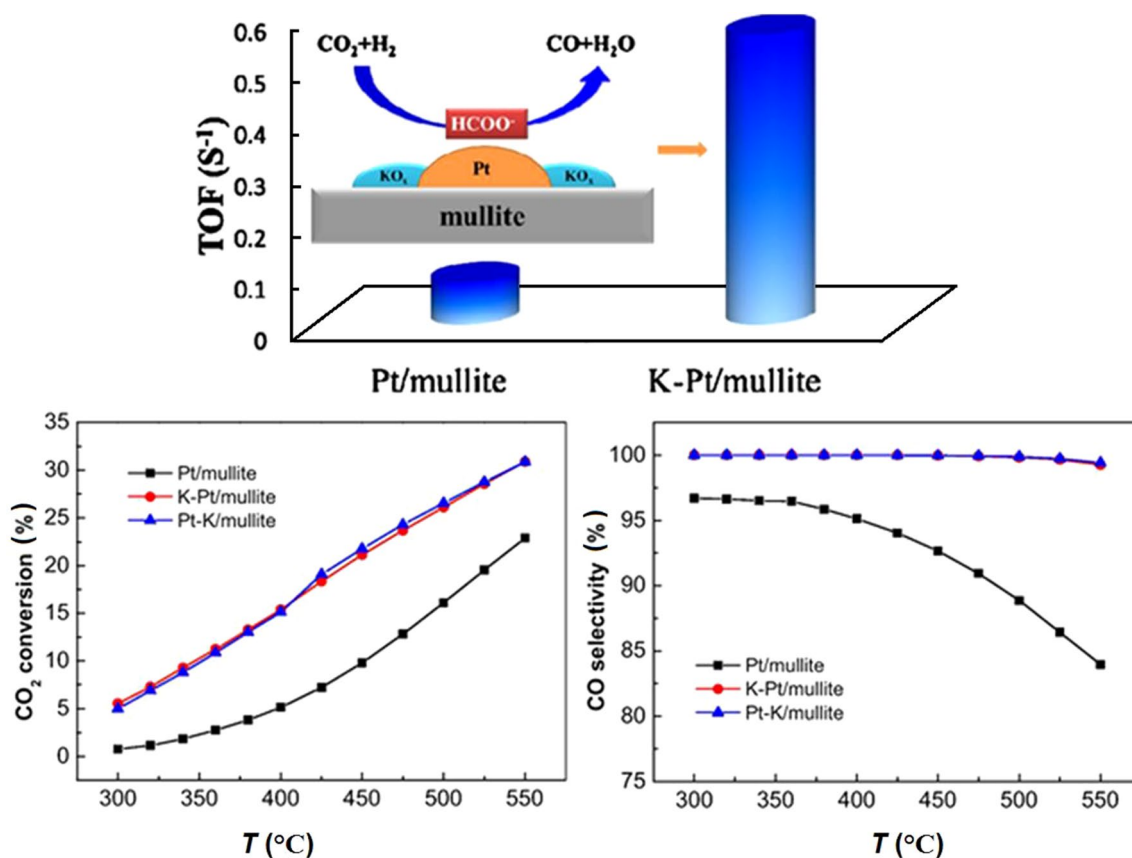
Fig. 13 Comparison of the turnover frequency (TOF) and the catalytic activity of RWGS reaction on Pt/mullite and Pt-K/mullite catalysts. Reaction conditions: 0.1 g of catalyst, 340 °C, 0.1 MPa, H$_2$/CO$_2$/N$_2$ = 4.5/4.5/1, feed flow rate of 50 mL/min [70]

enhance the activity and selectivity of the RWGS reaction. These strategies include varying support, tuning metal–support interactions, adding reducible transition metal oxide promoters, forming bimetallic alloys, adding alkali metals, and enveloping metal particles. The analysis of these advances suggests that enhancing CO$_2$ adsorption and facilitating CO desorption appear to be the key factors for enhancing CO$_2$ conversion and CO selectivity.

Although significant efforts have been made, studies have shown that the RWGS reaction is accompanied with a methanation side reaction on various catalysts. As a result, a mixture of CO and CH$_4$ products forms, thereby burdening subsequent separation processes. Thus, RWGS catalysts with 100% CO selectivity should be designed. In the future, combining different metals with supports/promoters and tailoring the fine structure of supported metal catalysts should be considered the important directions for designing highly selective catalysts of the RWGS reaction.

Future work may focus on the reaction mechanism of catalysts in a RWGS reaction. The reaction mechanism and even active sites have been strongly debated, and these aspects are essential for the rational design of highly efficient and selective RWGS catalysts. With the development of in situ and operando spectroscopy technologies, such as in situ XPS and in situ XRD, as well as the capability of DFT calculations, the reaction mechanism on various catalysts operating under various reaction conditions may be clarified in the future. With better understanding on the reaction mechanism and structure–activity/selectivity relationship, more efficient catalysts may be designed in the future.

Future work may also focus on the stability of catalysts in a RWGS reaction. The stability of catalysts in this reaction has been rarely explored. Several stability tests have been performed under conditions near the thermodynamic equilibrium of CO$_2$ conversion, which may mask the unstable nature of catalysts. The stability of catalysts is an important issue for a commercial process, so this parameter should be extensively investigated. Understanding the deactivation mechanism may also provide useful information for the rational design of stable catalysts in the RWGS reaction.
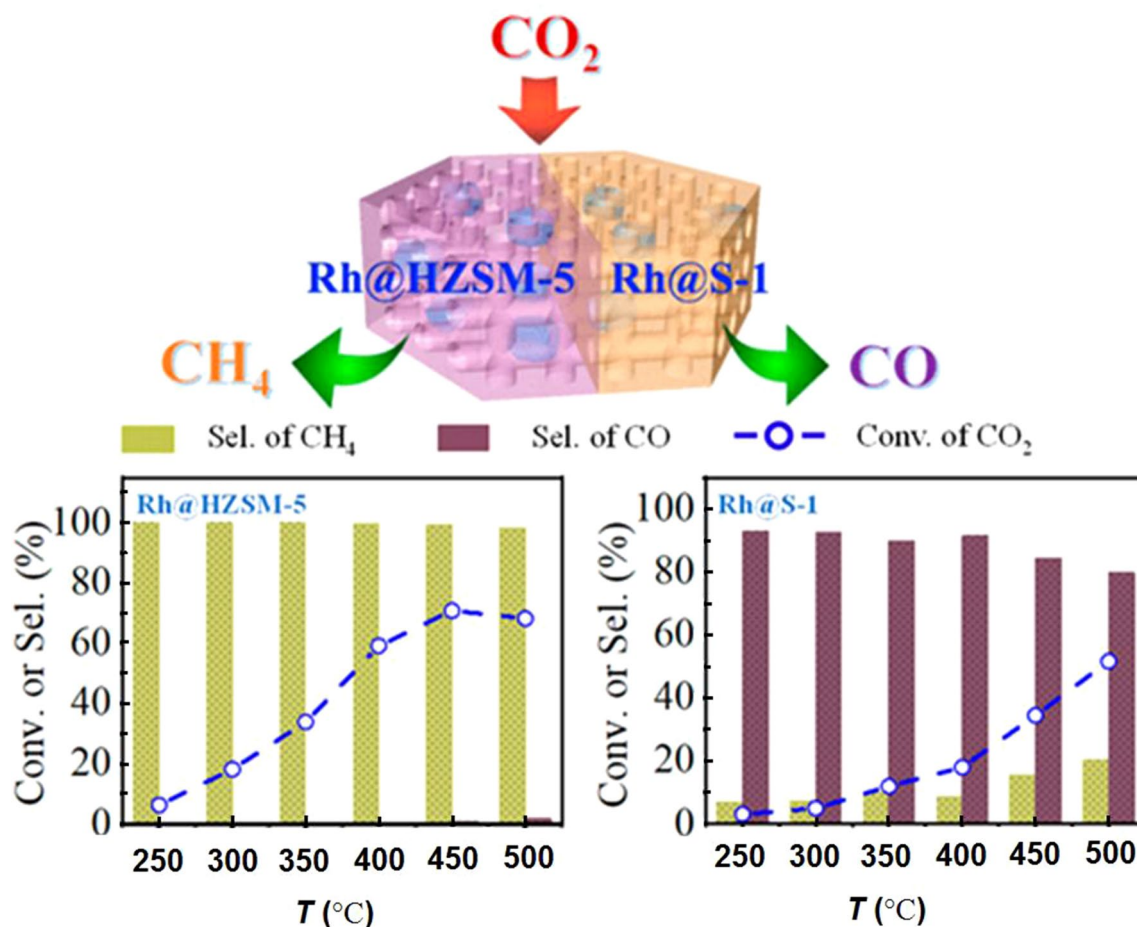
Fig. 14 Schematic of Rh enveloped in HZSM-5 (Rh@HZSM-5) and pure silica zeolite of S-1 (Rh@S-1) catalysts, and the conversion, CH_4 selectivity and CO selectivity as a function of reaction tempera- ture during CO_2 reduction. Reaction conditions: 0.5 g of catalyst, 1 MPa, $H_2/CO_2/Ar = 3/1/1$, feed flow rate of 30 mL/min [72]

References

1. Knutson TR, Tuleya RE (2004) Impact of CO_2-induced warming on simulated hurricane intensity and precipitation: sensitivity to the choice of climate model and convective parameterization. J Climate 17(18):3477–3495
2. Hansen J, Sato M, Ruedy R et al (2006) Global temperature change. Proc Natl Acad Sci USA 103(39):14288–14293
3. Yang J, Cai W, Ma MD et al (2020) Driving forces of China's CO_2 emissions from energy consumption based on Kaya-LMDI methods. Sci Total Environ 711:134569
4. Ahmed R, Liu GJ, Yousaf B et al (2020) Recent advances in carbon-based renewable adsorbent for selective carbon dioxide capture and separation—a review. J Clean Prod 242:118409
5. Ansaloni L, Salas-Gay J, Ligi S et al (2017) Nanocellulose- based membranes for CO_2 capture. J Membr Sci 522:216–225
6. Quarton CJ, Samsatli S (2020) The value of hydrogen and car- bon capture, storage and utilisation in decarbonising energy: insights from integrated value chain optimisation. Appl Energy 257:113936

7. Mac Dowell N, Fennell PS, Shah N et al (2017) The role of CO_2 capture and utilization in mitigating climate change. Nat Clim Change 7(4):243–249

8. Hadjadj R, Deák C, Palotás ÁB et al (2019) Renewable energy and raw materials—the thermodynamic support. J Clean Prod 241:118221

9. De Ras K, van de Vijver R, Galvita VV et al (2019) Carbon capture and utilization in the steel industry: challenges and opportunities for chemical engineering. Curr Opin Chem Eng 26:81–87

10. Wang ZJ, Song H, Liu HM et al (2020) Coupling of solar energy and thermal energy for carbon dioxide reduction: status and prospects. Angew Chem Int Ed 59:2–22

11. Kaiser P, Unde R, Kern C et al (2013) Production of liquid hydrocarbons with CO_2 as carbon source based on reverse water-gas shift and Fischer-tropsch synthesis. Chemie Ingenieur Tech 85(4):489–499

12. Daza YA, Kuhn JN (2016) CO_2 conversion by reverse water gas shift catalysis: comparison of catalysts, mechanisms and their consequences for CO_2 conversion to liquid fuels. RSC Adv 6(55):49675–49691

13. Ali N, Bilal M, Nazir MS et al (2020) Thermochemical and electrochemical aspects of carbon dioxide methanation: a sustainable approach to generate fuel via waste to energy theme. Sci Total Environ 712:136482

14. Zhuang YC, Currie R, McAuley KB et al (2019) Highly-selective CO_2 conversion via reverse water gas shift reaction over the 0.5 wt% Ru-promoted $Cu/ZnO/Al_2O_3$ catalyst. Appl Catal A: Gen 575:74–86

15. He YL, Yang KR, Yu ZW et al (2019) Catalytic manganese oxide nanostructures for the reverse water gas shift reaction. Nanoscale 11(35):16677–16688

16. Xu XD, Moulijn JA (1996) Mitigation of CO_2 by chemical conversion: plausible chemical reactions and promising products. Energy Fuels 10(2):305–325

17. Xu JH, Su X, Duan HM et al (2016) Influence of pretreatment temperature on catalytic performance of rutile TiO_2-supported ruthenium catalyst in CO_2 methanation. J Catal 333:227–237

18. Nityashree N, Price CAH, Pastor-Perez L et al (2020) Carbon stabilised saponite supported transition metal-alloy catalysts for chemical CO_2 utilisation via reverse water-gas shift reaction. Appl Catal B: Environ 261:118241

19. Dias YR, Perez-Lopez OW (2020) Carbon dioxide methanation over Ni-Cu/SiO₂ catalysts. Energy Convers Manag 203:112214

20. Konsolakis M, Lykaki M, Stefa S et al (2019) CO_2 hydrogenation over nanoceria-supported transition metal catalysts: role of ceria morphology (nanorods versus nanocubes) and active phase nature (Co versus Cu). Nanomaterials 9(12):1739

21. Wang YJ, Xu Y, Liu QK et al (2019) Enhanced low-temperature activity for CO_2 methanation over NiMgAl/SiC composite catalysts. J Chem Technol Biotechnol 94(12):3780–3786

22. Qiu M, Tao HL, Li Y et al (2019) Insight into the mechanism of CO_2 and CO methanation over Cu(100) and Co-modified Cu(100) surfaces: a DFT study. Appl Surf Sci 495:143457

23. Li WH, Zhang GH, Jiang X et al (2019) CO_2 hydrogenation on unpromoted and M-promoted Co/TiO_2 catalysts (M = Zr, K, Cs): effects of crystal phase of supports and metal–support interaction on tuning product distribution. ACS Catal 9(4):2739–2751

24. Ginés MJL, Marchi AJ, Apesteguía CR (1997) Kinetic study of the reverse water-gas shift reaction over $CuO/ZnO/Al_2O_3$ catalysts. Appl Catal A: Gen 154(1–2):155–171

25. Fujita SI, Usui M, Takezawa N (1992) Mechanism of the reverse water gas shift reaction over Cu/ZnO catalyst. J Catal 134(1):220–225

26. Chen C, Cheng WH, Lin S (2000) Mechanism of CO formation in reverse water-gas shift reaction over Cu/Al_2O_3 catalyst. Catal Lett 68(1–2):45–48

27. Goguet A, Meunier FC, Tibiletti D et al (2004) Spectrokinetic investigation of reverse water-gas-shift reaction intermediates over a Pt/CeO_2 catalyst. J Phys Chem B 108(52):20240–20246

28. Zhang M, Zijlstra B, Filot IAW et al (2020) A theoretical study of the reverse water-gas shift reaction on Ni(111) and Ni(311) surfaces. Can J Chem Eng 98(3):740–748

29. Fornero EL, Chiavassa DL, Bonivardi AL et al (2017) Transient analysis of the reverse water gas shift reaction on Cu/ZrO_2 and $Ga_2O_3/Cu/ZrO_2$ catalysts. J CO_2 Util 22:289–298

30. Ernst K (1992) Kinetics of the reverse water–gas shift reaction over Cu(110). J Catal 134(1):66–74

31. Hadden RA, Vandervell HD, Waugh KC et al (1988) The adsorption and decomposition of carbon dioxide on polycrystalline copper. Catal Lett 1(1–3):27–33

32. Kim SS, Lee HH, Hong SC (2012) A study on the effect of support's reducibility on the reverse water-gas shift reaction over Pt catalysts. Appl Catal A: Gen 423–424:100–107

33. Widmann D, Behm RJ (2011) Active oxygen on a Au/TiO_2 catalyst: formation, stability, and CO oxidation activity. Angew Chem Int Ed 50(43):10241–10245

34. Kotobuki M, Leppelt R, Hansgen DA et al (2009) Reactive oxygen on a Au/TiO_2 supported catalyst. J Catal 264(1):67–76

35. Sharma S, Hilaire S, Vohs JM et al (2000) Evidence for oxidation of ceria by CO_2. J Catal 190(1):199–204

36. Bernal S, Blanco G, Gatica JM et al (2001) Effect of mild Re-oxidation treatments with CO_2 on the chemisorption capability of a Pt/CeO_2 catalyst reduced at 500 °C. J Catal 200(2):411–415

37. Su X, Yang XL, Zhao B et al (2017) Designing of highly selective and high-temperature endurable RWGS heterogeneous catalysts: recent advances and the future directions. J Energy Chem 26(5):854–867

38. Chen XD, Su X, Liang BL et al (2016) Identification of relevant active sites and a mechanism study for reverse water gas shift reaction over Pt/CeO_2 catalysts. J Energy Chem 25(6):1051–1057

39. Jacobs G, Davis BH (2005) Reverse water-gas shift reaction: steady state isotope switching study of the reverse water-gas shift reaction using in situ DRIFTS and a Pt/ceria catalyst. Appl Catal A: Gen 284(1–2):31–38

40. Shido T, Iwasawa Y (1993) Reactant-promoted reaction mechanism for water-gas shift reaction on Rh-doped CeO_2. J Catal 141(1):71–81

41. Chen XD, Su X, Duan HM et al (2017) Catalytic performance of the Pt/TiO_2 catalysts in reverse water gas shift reaction: controlled product selectivity and a mechanism study. Catal Today 281:312–318

42. Kim SS, Park KH, Hong SC (2013) A study of the selectivity of the reverse water–gas-shift reaction over Pt/TiO_2 catalysts. Fuel Process Technol 108:47–54

43. Meunier FC, Tibiletti D, Goguet A et al (2005) On the reactivity of carbonate species on a Pt/CeO_2 catalyst under various reaction atmospheres: application of the isotopic exchange technique. Appl Catal A: Gen 289(1):104–112

44. Goguet A, Shekhtman S, Burch R et al (2006) Pulse-response TAP studies of the reverse water–gas shift reaction over a Pt/CeO_2 catalyst. J Catal 237(1):102–110

45. Dou J, Sheng Y, Choong C et al (2017) Silica nanowires encapsulated Ru nanoparticles as stable nanocatalysts for selective hydrogenation of CO_2 to CO. Appl Catal B: Environ 219:580–591

46. Panagiotopoulou P (2017) Hydrogenation of CO_2 over supported noble metal catalysts. Appl Catal A: Gen 542:63–70

47. Park JN, McFarland EW (2009) A highly dispersed Pd–Mg/SiO₂ catalyst active for methanation of CO_2. J Catal 266(1):92–97

48. Porosoff MD, Yan BH, Chen JG (2016) Catalytic reduction of CO_2 by H_2 for synthesis of CO, methanol and hydrocarbons: challenges and opportunities. Energy Environ Sci 9(1):62–73

49. Saeidi S, Najari S, Fazlollahi F et al (2017) Mechanisms and kinetics of CO_2 hydrogenation to value-added products: a detailed review on current status and future trends. Renew Sustain Energy Rev 80:1292–1311

50. Wang W, Wang SP, Ma XB et al (2011) Recent advances in catalytic hydrogenation of carbon dioxide. Chem Soc Rev 40(7):3703–3727

51. Kattel S, Liu P, Chen JG (2017) Tuning selectivity of CO_2 hydrogenation reactions at the metal/oxide interface. J Am Chem Soc 139(29):9739–9754

52. Tao Y, Zhu YM, Liu CJ et al (2018) A highly selective Cr/ZrO_2 catalyst for the reverse water-gas shift reaction prepared from simulated Cr-containing wastewater by a photocatalytic deposition process with ZrO_2. J Environ Chem Eng 6(6):6761–6770

53. Porosoff MD, Yang XF, Boscoboinik JA et al (2014) Molybdenum carbide as alternative catalysts to precious metals for highly selective reduction of CO_2 to CO. Angew Chem Int Ed 53(26):6705–6709

54. Daza YA, Maiti D, Kent RA et al (2015) Isothermal reverse water gas shift chemical looping on $La_{0.75}Sr_{0.25}Co_{(1-Y)}Fe_YO_3$ perovskite-type oxides. Catal Today 258:691–698

55. Aitbekova A, Wu LH, Wrasman CJ et al (2018) Low-temperature restructuring of CeO_2-supported Ru nanoparticles determines selectivity in CO_2 catalytic reduction. J Am Chem Soc 140(42):13736–13745

56. Matsubu JC, Yang VN, Christopher P (2015) Isolated metal active site concentration and stability control catalytic CO_2 reduction selectivity. J Am Chem Soc 137(8):3076–3084

57. Li J, Lin YP, Pan XL et al (2019) Enhanced CO_2 methanation activity of Ni/anatase catalyst by tuning strong metal–support interactions. ACS Catal 9(7):6342–6348

58. Kattel S, Yan BH, Chen JG et al (2016) CO_2 hydrogenation on Pt, Pt/SiO_2 and Pt/TiO_2: importance of synergy between Pt and oxide support. J Catal 343:115–126

59. Ye JY, Ge QF, Liu CJ (2015) Effect of PdIn bimetallic particle formation on CO_2 reduction over the $Pd-In/SiO_2$ catalyst. Chem Eng Sci 135:193–201

60. Shi C, O'Grady CP, Peterson AA et al (2013) Modeling CO_2 reduction on Pt(111). Phys Chem Chem Phys 15(19):7114

61. Kwak JH, Kovarik L, Szanyi J (2013) Heterogeneous catalysis on atomically dispersed supported metals: CO_2 reduction on multifunctional Pd catalysts. ACS Catal 3(9):2094–2100

62. Bobadilla LF, Santos JL, Ivanova S et al (2018) Unravelling the role of oxygen vacancies in the mechanism of the reverse water–gas shift reaction by operando DRIFTS and ultraviolet–visible spectroscopy. ACS Catal 8(8):7455–7467

63. Yang SC, Pang SH, Sulmonetti TP et al (2018) Synergy between ceria oxygen vacancies and Cu nanoparticles facilitates the catalytic conversion of CO_2 to CO under mild conditions. ACS Catal 8(12):12056–12066

64. Sakurai H, Tsubota S, Haruta M (1993) Hydrogenation of CO_2 over gold supported on metal oxides. Appl Catal A: Gen 102(2):125–136

65. Kattel S, Yu WT, Yang XF et al (2016) CO_2 hydrogenation over oxide-supported PtCo catalysts: the role of the oxide support in determining the product selectivity. Angew Chem Int Ed 55(28):7968–7973

66. Kwak JH, Kovarik L, Szanyi J (2013) CO_2 reduction on supported Ru/Al_2O_3 catalysts: cluster size dependence of product selectivity. ACS Catal 3(11):2449–2455

67. Li SW, Xu Y, Chen YF et al (2017) Tuning the selectivity of catalytic carbon dioxide hydrogenation over iridium/cerium oxide catalysts with a strong metal–support interaction. Angew Chem Int Ed 56(36):10761–10765

68. Yan BH, Zhao BH, Kattel S et al (2019) Tuning CO_2 hydrogenation selectivity via metal-oxide interfacial sites. J Catal 374:60–71

69. Chen CS, Cheng WH, Lin SS (2003) Study of reverse water gas shift reaction by TPD, TPR and CO_2 hydrogenation over potassium-promoted Cu/SiO_2 catalyst. Appl Catal A: Gen 238(1):55–67

70. Liang BL, Duan HM, Su X et al (2017) Promoting role of potassium in the reverse water gas shift reaction on Pt/mullite catalyst. Catal Today 281:319–326

71. Bando KK, Soga K, Kunimori K et al (1998) Effect of Li additive on CO_2 hydrogenation reactivity of zeolite supported Rh catalysts. Appl Catal A: Gen 175(1–2):67–81

72. Wang CT, Guan EJ, Wang L et al (2019) Product selectivity controlled by nanoporous environments in zeolite crystals enveloping rhodium nanoparticle catalysts for CO_2 hydrogenation. J Am Chem Soc 141(21):8482–8488

73. Goguet A, Meunier F, Breen J et al (2004) Study of the origin of the deactivation of a Pt/CeO_2 catalyst during reverse water gas shift (RWGS) reaction. J Catal 226(2):382–392

74. Wang LC, Tahvildar Khazaneh M, Widmann D et al (2013) TAP reactor studies of the oxidizing capability of CO_2 on a Au/CeO_2 catalyst—a first step toward identifying a redox mechanism in the Reverse Water-Gas Shift reaction. J Catal 302:20–30

75. Jin T, Zhou Y, Mains GJ et al (1987) Infrared and X-ray photoelectron spectroscopy study of carbon monoxide and carbon dioxide on platinum/ceria. J Phys Chem 91(23):5931–5937

76. Porosoff MD, Chen JG (2013) Trends in the catalytic reduction of CO_2 by hydrogen over supported monometallic and bimetallic catalysts. J Catal 301:30–37

77. Chen XD, Su X, Su HY et al (2017) Theoretical insights and the corresponding construction of supported metal catalysts for highly selective CO_2 to CO conversion. ACS Catal 7(7):4613–4620

78. Kim SS, Lee HH, Hong SC (2012) The effect of the morphological characteristics of TiO_2 supports on the reverse water–gas shift reaction over Pt/TiO_2 catalysts. Appl Catal B: Environ 119–120:100–108

79. Ro I, Sener CN, Stadelman TM et al (2016) Measurement of intrinsic catalytic activity of Pt monometallic and $Pt-MoO_x$ interfacial sites over visible light enhanced $PtMoO_x/SiO_2$ catalyst in reverse water gas shift reaction. J Catal 344:784–794

80. Alayoglu S, Beaumont SK, Zheng F et al (2011) CO_2 hydrogenation studies on Co and CoPt bimetallic nanoparticles under reaction conditions using TEM. XPS NEXAFS. Top Catal 54(13–15):778–785

81. Yuan HJ, Zhu XL, Han JY et al (2018) Rhenium-promoted selective CO_2 methanation on Ni-based catalyst. J CO_2 Util 26:8–18

82. Kharaji AG, Shariati A, Takassi MA (2013) A novel γ-alumina supported Fe-Mo bimetallic catalyst for reverse water gas shift reaction. Chin J Chem Eng 21(9):1007–1014

83. Zhu XL, Shen M, Lobban LL et al (2011) Structural effects of Na promotion for high water gas shift activity on $Pt–Na/TiO_2$. J Catal 278(1):123–132

84. Santos J, Bobadilla L, Centeno M et al (2018) Operando DRIFTS-MS study of WGS and rWGS reaction on biochar-based Pt catalysts: the promotional effect of Na. C 4(3):47

85. Yang M, Li S, Wang Y et al (2014) Catalytically active Au-$O(OH)_x$-species stabilized by alkali ions on zeolites and mesoporous oxides. Science 346(6216):1498–1501

86. Yang XL, Su X, Chen XD et al (2017) Promotion effects of potassium on the activity and selectivity of Pt/zeolite catalysts for reverse water gas shift reaction. Appl Catal B: Environ 216:95–105

Dr. Xinli Zhu is a professor at the School of Chemical Engineering and Technology, Tianjin University. He received his BS in Chemical Engineering in 2002 and Ph.D in 2007 from Tianjin University. He was a postdoctoral research fellow at the University of Oklahoma in 2007–2011. He joined Tianjin University in 2011. His research interest includes the catalytic conversion of biomass-derived oxygenates to chemicals and fuels by using combined experimental and theoretical approaches.